

## Implementation of the strongly pronounced non-linear viscoelasticity of an incompressible filled rubber

T. Scheffer, F. Goldschmidt, S. Diebels

*Filled rubber materials regularly show a pronounced non-linear viscoelasticity with very long relaxation times. In this contribution, a phenomenological description for an incompressible carbon black-filled EPDM (ethylene propylene diene monomer) is given, which also shows the abovementioned characteristic behaviour. In order to represent the non-linear viscoelastic material, the relaxation times of the model are chosen not as constant material parameters but as process-dependent functions.*

*This contribution presents two different realisations of the model's implementation. At first, this work provides an implementation of the material model, which is able to describe complex geometries and loading conditions. In this realisation, the three-dimensional model is implemented in the open source finite element library deal.II for finite deformations. Hence, real applications can be represented. In an alternative numerical solution, the model is reduced to the single case of uniaxial tension. The model is simplified to scalar equations, which are quite easy to handle for the implementation. This procedure provides a more simple identification process, but it presents the problem that the model character is extremely restricted for the individual case of uniaxial tension.*

*For the numerical realisation, at first, special attention has to be turned on the determination of the inelastic part of the kinematics. A detailed evaluation of the necessary evolution equations is provided in this contribution. Finally, the results of the different implementations are compared with respect to different loading conditions, like relaxation tests or cyclic loading.*

### 1 Introduction

Filled rubber as a construction material is of great interest for a wide field of industrial sections such as the automotive industry. Since there are so many combinations of different natural rubbers, various filler materials and their concentrations, a huge range of properties, which are important for the specific application, can be achieved. Hence, the resulting wide range of possible applications causes a high interest in the research of these materials. Only a few papers dealing with this topic should be named exemplarily, e. g. Besdo and Ihlemann (2003); Dannenberg (1975); Hartmann et al. (2003); Keck (1998); Lion (1996, 2004); Miehe and Keck (2000).

Usually, the behaviour of highly filled elastomers is complex to describe due to its time- and process-dependence. It is caused by the complex behaviour of rubber matrix materials as well as of the interaction of filler particles with themselves and with the matrix material. Characteristic for the complex behaviour of filled elastomers is the existence of very long relaxation times ranging from several hours to several days even. This effect can be seen in relaxation experiments for varying deformation levels. The appearance of these long relaxation times also results in a hysteresis loop for cyclic loading conditions, which can still be seen in the experiment when using the slowest possible machine speeds. This effect is modelled by Kaliske and Rothert (1998) and Lion (2000) with a plasticity theory, whereas a non-linear viscoelastic model with sufficiently large relaxation times is also able to describe the observed material behaviour as can be seen in Koprowski-Theiß et al. (2011a) or Scheffer et al. (2013).

The investigated incompressible carbon black-filled EPDM shows exactly these characteristic effects and is described in a purely phenomenological way. The step-by-step development of the macroscopic model of this material is provided in another article by Scheffer et al. (2013) for finite deformations, at first, starting with the basic elasticity. Furthermore, the inclusion of the viscoelasticity for moderate strain rates in cyclic tests and the relaxation behaviour in the material model is described.

As a first numerical method, the original model in its formulation according to large deformations, which provides the complete three-dimensional information without any simplification, is implemented. The presented numerical treatment is realised in an open source finite element library called deal.II, cf. Bangerth et al. (2007, 2013). It allows complete insight and intervention in the model's structure, whereby the simulation of this quite complex model is time-consuming especially according to parameter identification. In order to simplify the simulation and

to shorten time, the material model can be specified for the uniaxial tension test allowing the simplification to scalar equations but also limiting the range of the material model's potential to a very special case, in this case, the behaviour of the material with respect to uniaxial deformation. However, in real industrial applications, the deformation of a system assembly usually is multiaxial. The deformation values, their direction and the deformation rates of an assembly can vary a lot from one material point to the other due to multiple external forces as well as due to its geometry; the material behaviour of filled rubber is usually sensitive on all these points. In order to describe such multiaxial loadings, Jöhlitz and Diebels (2011) or Seibert et al. (2014) have considered that experimental multiaxial data has to be made available to identify the model parameters.

## 2 Material description of a carbon black-filled EPDM

### 2.1 Samples and experimental device

For filled rubber materials, the bulk modulus usually is several orders higher than the shear modulus, besides it has a porous structure. In the case of the presented contribution, the investigated material is an incompressible and isotropic EPDM (ethylene propylene diene monomer). It is commercially available and die-cut directly out of a car door gasket consisting of an incompressible part and the foamed part, which is structurally compressible. The pure solid part as well as the foamed part of the assembly consist of the same matrix material. This article only deals with the solid material without pores. For the description of the porous part, the reader is referred to the work of Koprowski-Theiß et al. (2011b, 2012a,b). The current description is accomplished with respect to uniaxial tension data. In the parameter identification strain rates in the order of  $10^{-3} \text{ s}^{-1}$  to  $10^{-1} \text{ s}^{-1}$  are taken into account, whereby the provided model in the following shall also be applicable to represent the material behaviour in a larger range.

### 2.2 Material model

The procedure for the development of the material model for the EPDM is purely phenomenological describing the behaviour that can be seen in the experiments and the observed effects within. There are many articles dealing with the topic of finite viscoelasticity. Hence, it is not possible to name all of them, nevertheless some of them shall be quoted exemplarily in this contribution, e. g. Amin et al. (2006, 2010); Haupt (2000); Haupt and Lion (2002); Laiarinandrasana et al. (2003); Lion (2000); Reese (2000); Reese and Govindjee (1998); Sedlan (2001). According to the investigated material, this contribution only provides the resulting material model. For details of the modelling process, the reader is referred to another article of Scheffer et al. (2013). Only a brief summary of the results is provided in the following section.

The composition of the material model is based on a rheological interpretation. The rheological model contains a spring, which is arranged in parallel to  $j = 1 \dots n$  Maxwell elements with each of the Maxwell elements consisting of a spring connected in series to a dashpot, cf. Fig. 1. Herein, the single spring represents the equilibrium stiffness,

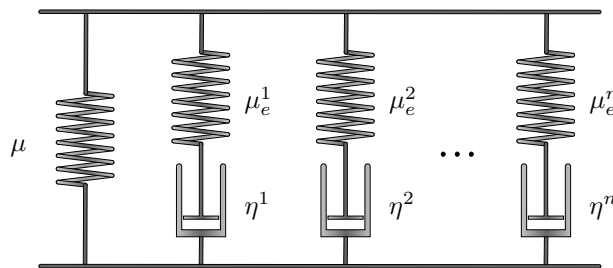


Figure 1: Rheological model of the viscoelastic behaviour with  $n$  Maxwell elements.

whereas the Maxwell elements describe the viscoelastic effects. For the kinematical consideration of finite strains, a multiplicative split of the deformation gradient  $\mathbf{F}$  into an elastic part  $\mathbf{F}_e^j$  and an inelastic part  $\mathbf{F}_i^j$

$$\mathbf{F} = \mathbf{F}_e^j \cdot \mathbf{F}_i^j \quad (1)$$

is executed for each Maxwell element  $j = 1 \dots n$ . For every single branch of the rheological model, an additional fictitious intermediate configuration has to be introduced, which has been used by Kröner (1959) and Lee (1969)

in plasticity theory at first. For more details of the theory, see e. g. Jhohltz (2009); Koprowski-Theiß (2011); Lion (1996, 2000); Sedlan (2001). Additionally, an overview of several hyperelastic models for rubber-like materials is given in the work of Marckmann and Verron (2006), which promotes the approach by a phenomenological strategy formulated by a polynomial series, introduced by Rivlin and Saunders (1951)

$$\rho_0 \Psi = \sum_{k,l=0}^{N,M} c_{kl} (\text{I} - 3)^k (\text{II} - 3)^l. \quad (2)$$

Therein, the order of the first and second invariant parts of the corresponding deformation tensor, e. g. the left Cauchy-Green deformation tensor  $\mathbf{B}$ , is varied with respect to the experimental observations to be represented. In case of  $\mathbf{B}$ , the corresponding invariants are

$$\begin{aligned} \text{I}_{\mathbf{B}} &= \text{tr } \mathbf{B} = \mathbf{B} : \mathbf{I}, \\ \text{II}_{\mathbf{B}} &= \frac{1}{2} ((\mathbf{B} : \mathbf{I})^2 - \mathbf{B}^T : \mathbf{B}). \end{aligned} \quad (3)$$

An important requirement to be satisfied is the Clausius-Planck inequality

$$p \mathbf{I} : \mathbf{D} + \mathbf{T} : \mathbf{D} - \rho \dot{\Psi} \geq 0, \quad (4)$$

in which  $p$  stands for the Lagrangian multiplier, representing the incompressibility,  $\mathbf{D}$  for the deformation velocity, and  $\mathbf{I}$  for the 2<sup>nd</sup> rank identity tensor. As introduced later, the process variables for the given material model are

$$\mathcal{S} = \{ \mathbf{B}, \mathbf{B}_e^j, \mathbf{D} \}. \quad (5)$$

In this set of variables the left Cauchy-Green deformation tensor  $\mathbf{B} = \mathbf{F} \cdot \mathbf{F}^T$  represents the strain of the single equilibrium spring and  $\mathbf{B}_e^j = \mathbf{F}_e^j \cdot (\mathbf{F}_e^j)^T$  the elastic deformation of the spring in the  $j^{\text{th}}$  Maxwell element. Furthermore, in the introduced model, the stress depends on the deformation velocity  $\mathbf{D}$ . Taking into account the principle of equipresence (cf. Truesdell and Toupin (1960); Truesdell and Noll (2004)), at first, it has to be observed, if  $\mathbf{D}$  has any influence on the evaluation of the Clausius-Planck inequality. The derivation of  $\Psi$  results in

$$\dot{\Psi}(\mathbf{B}, \mathbf{B}_e^j, \mathbf{D}) = \frac{\partial \Psi(\mathbf{B}, \mathbf{B}_e^j, \mathbf{D})}{\partial \mathbf{B}} : \dot{\mathbf{B}} + \sum_{j=1}^n \frac{\partial \Psi(\mathbf{B}, \mathbf{B}_e^j, \mathbf{D})}{\partial \mathbf{B}_e^j} : \dot{\mathbf{B}}_e^j + \frac{\partial \Psi(\mathbf{B}, \mathbf{B}_e^j, \mathbf{D})}{\partial \mathbf{D}} : \dot{\mathbf{D}}. \quad (6)$$

Since  $\dot{\mathbf{D}}$  is no process variable

$$\frac{\partial \Psi(\mathbf{B}, \mathbf{B}_e^j, \mathbf{D})}{\partial \mathbf{D}} : \dot{\mathbf{D}} \quad (7)$$

vanishes according to the considerations of de Boer and Ehlers (1986) and Bowen (1976). The free energy does not depend on the deformation velocity  $\mathbf{D}$ . So, in the following, the free energy function  $\Psi$  is split into an equilibrium and  $n$  non-equilibrium parts

$$\Psi = \Psi_{eq}(\mathbf{B}) + \sum_{j=1}^n \Psi_{neq}^j(\mathbf{B}_e^j), \quad (8)$$

only depending on  $\mathbf{B}$  and  $\mathbf{B}_e^j$ . This corresponds to the additive composition of the stresses in the branches of the rheological model (cf. Fig. 1)

$$\mathbf{T} = \mathbf{T}_{eq}(\mathbf{B}) + \sum_{j=1}^n \mathbf{T}_{neq}^j(\mathbf{B}_e^j). \quad (9)$$

The Clausius-Planck inequality (4) results in

$$\begin{aligned} & \left( \mathbf{T} + p \mathbf{I} - 2 J^{-1} \rho_0 \mathbf{B} \cdot \frac{\partial \Psi_{eq}}{\partial \mathbf{B}} - \sum_{j=1}^n 2 J^{-1} \rho_0 \mathbf{B}_e^j \cdot \frac{\partial \Psi_{neq}^j}{\partial \mathbf{B}_e^j} \right) : \mathbf{D} \\ & + \sum_{j=1}^n \left( 2 J^{-1} \rho_0 \frac{\partial \Psi_{neq}^j}{\partial \mathbf{B}_e^j} \right) : \mathbf{F}_e^j \cdot \overset{\Delta}{\Gamma}_i^j \cdot (\mathbf{F}_e^j)^T \geq 0, \end{aligned} \quad (10)$$

with the inelastic deformation rate of the intermediate configuration  $\overset{\Delta}{\Gamma}_i^j$ . The material is considered incompressible, so  $J = \det \mathbf{F}$  equals 1. The first summand of this inequality can be evaluated with respect to Coleman and Noll (1963) leading to the constitutive relation for the Cauchy stress  $\mathbf{T}$

$$\mathbf{T} = -p \mathbf{I} + 2 \rho_0 \mathbf{B} \frac{\partial \Psi_{eq}}{\partial \mathbf{B}} + \sum_{j=1}^n 2 \rho_0 \mathbf{B}_e^j \cdot \frac{\partial \Psi_{neq}^j}{\partial \mathbf{B}_e^j}. \quad (11)$$

The basis of the material model is represented by the equilibrium stress in the single spring. A big problem, which occurs during the experiment, is that the way to reach the equilibrium stress is quite complex due to the long relaxation times of several hours or even more, which are characteristic for different filled rubber materials. Classical methods like cyclic deformations up to a maximum deformation with very slow strain rates or stepwise relaxation tests for different strain levels are not reliable for these materials. An alternative experimental process has to be developed. Sedlan (2001) has observed that a cyclic pretreatment around the middle strain of interest results in a decrease of the resulting hysteresis loops until a stationary condition is achieved. A subsequent relaxation test reaches the equilibrium stress in a short time of only some minutes leading to faster and effectively reproducible experiments, shown in the investigations of Scheffer et al. (2013). The resulting basic elasticity shows a characteristic *S*-shaped stress-strain relation and is represented by a Yeoh-approach, provided by Yeoh (1993) and Yeoh and Fleming (1997)

$$\rho_0 \Psi_{eq}(\mathbf{I}_B) = c_{10} (\mathbf{I}_B - 3) + c_{20} (\mathbf{I}_B - 3)^2 + c_{30} (\mathbf{I}_B - 3)^3. \quad (12)$$

In order to represent the non-linear viscoelasticity, four Maxwell elements are necessary. The specific free energy for these elements is formulated in relation to the invariant of the elastic left Cauchy-Green deformation  $\mathbf{B}_e^j$  for each Maxwell element's spring. For the first element, the free energy is chosen as

$$\rho_0 \Psi_{neq}^1(\mathbf{I}_{B_e^1}) = c_{301} (\mathbf{I}_{B_e^1} - 3)^3. \quad (13)$$

and, for the remaining three Maxwell elements, a Neo-Hookean approach

$$\rho_0 \Psi_{neq}^j(\mathbf{I}_{B_e^j}) = c_{10j} (\mathbf{I}_{B_e^j} - 3); \quad j = 2 \dots 4 \quad (14)$$

is chosen. With the free energies of the non-equilibrium parts, the resulting constitutive equation for  $\mathbf{T}$  is given by

$$\begin{aligned} \mathbf{T} = & -p \mathbf{I} + 2 [c_{10} + 2c_{20} (\mathbf{I}_B - 3) + 3c_{30} (\mathbf{I}_B - 3)^2] \mathbf{B} \\ & + 6c_{301} (\mathbf{I}_{B_e^1} - 3)^2 \mathbf{B}_e^1 + \sum_{j=2}^4 2c_{10j} \mathbf{B}_e^j, \end{aligned} \quad (15)$$

including both the equilibrium part of the Cauchy stress as well as the overstress. The remaining part of the Clausius-Planck inequality (10)

$$\begin{aligned} & \sum_{j=1}^n \left( 2\rho_0 \frac{\partial \Psi_{neq}^j}{\partial \mathbf{B}_e^j} \right) : \mathbf{F}_e^j \cdot \overset{\Delta}{\Gamma}_i^j \cdot (\mathbf{F}_e^j)^T \geq 0 \\ & \sum_{j=1}^n \left[ 2\rho_0 \left( \frac{\partial \Psi_{neq}^j}{\partial \mathbf{I}_{B_e^j}} \frac{d\mathbf{I}_{B_e^j}}{d\mathbf{B}_e^j} + \frac{\partial \Psi_{neq}^j}{\partial \Pi_{B_e^j}} \frac{d\Pi_{B_e^j}}{d\mathbf{B}_e^j} \right) \right] : \mathbf{F}_e^j \cdot \overset{\Delta}{\Gamma}_i^j \cdot (\mathbf{F}_e^j)^T \geq 0 \end{aligned} \quad (16)$$

is used for the evaluation of the inelastic deformation rates in the  $n$  Maxwell elements, referring to the conclusions made in Jöhlich (2009); Lion (2000) and Sedlan (2001). In the following, this contribution provides the development of the evolution equations in a general form for incompressible materials, according to the free energy approaches with respect to the formulation (2). It is not restricted to a specific model approach. The derivation of the kinematical evolution equations for the Maxwell elements is a major point in this article. It is given in a formulation, which is in such a general form, that different approaches for the specific free energy can be taken into account. Applying the derivatives of the invariants, in this case, for the example of  $\mathbf{B}_e^j$

$$\begin{aligned} \frac{d\mathbf{I}_{B_e^j}}{d\mathbf{B}_e^j} &= \mathbf{I}, \\ \frac{d\Pi_{B_e^j}}{d\mathbf{B}_e^j} &= \mathbf{I}_{B_e^j} \mathbf{I} - (\mathbf{B}_e^j)^T. \end{aligned} \quad (17)$$

Eq. (16) results in

$$\sum_{j=1}^n \underbrace{\left[ 2\rho_0 \left( \frac{\partial \Psi_{neq}^j}{\partial \mathbf{I}_{B_e^j}} \mathbf{C}_e^j + \frac{\partial \Psi_{neq}^j}{\partial \Pi_{B_e^j}} (\mathbf{I}_{B_e^j} \mathbf{C}_e^j - \mathbf{C}_e^j \cdot \mathbf{C}_e^j) \right) \right]}_{LHS} : \overset{\Delta}{\Gamma}_i^j \geq 0, \quad (18)$$

with the elastic right Cauchy-Green deformation tensor  $\mathbf{C}_e^j = (\mathbf{F}_e^j)^T \cdot \mathbf{F}_e^j$ . With the incompressibility condition

$$\det \mathbf{F} = \det \mathbf{F}_e = \det \mathbf{F}_i = 1, \quad (19)$$

it can be shown that

$$\text{tr}(\overset{\Delta}{\Gamma}_i^j) = 0. \quad (20)$$

Hence, the evolution equation for  $\overset{\Delta}{\Gamma}_i^j$  has to show a deviatoric form. In addition, the left-hand side (*LHS*) of the product in the inequality (18) has to be deviatoric, too. As considered in Haupt (2000), this inequality is fulfilled for isotropic behaviour in the case that the inelastic deformation rate  $\overset{\Delta}{\Gamma}_i^j$  is proportional to the left-hand side (*LHS*) of the product. Therefore, a proportionality factor  $\eta^j$  is introduced representing the viscosity of the  $j^{\text{th}}$  Maxwell element

$$\begin{aligned} \eta^j \overset{\Delta}{\Gamma}_i^j &= \left[ LHS - \frac{1}{3} \text{tr}(LHS) \mathbf{I} \right] \\ \overset{\Delta}{\Gamma}_i^j &= \frac{1}{\eta^j} \left[ LHS - \frac{1}{3} \text{tr}(LHS) \mathbf{I} \right]. \end{aligned} \quad (21)$$

The transport of the inelastic deformation rate  $\overset{\Delta}{\Gamma}_i^j$  of the inelastic intermediate configuration to the reference configuration is executed using the *pull back* operation

$$\dot{\mathbf{E}}_i^j = \frac{1}{2} \dot{\mathbf{C}}_i^j = (\mathbf{F}_i^j)^T \cdot \overset{\Delta}{\Gamma}_i^j \cdot \mathbf{F}_i^j \Leftrightarrow \overset{\Delta}{\Gamma}_i^j = \frac{1}{2} (\mathbf{F}_i^j)^{-T} \cdot \dot{\mathbf{C}}_i^j \cdot (\mathbf{F}_i^j)^{-1}. \quad (22)$$

The evaluation of the left-hand side (*LHS*) in (18) with (21) & (22) provides an evolution equation for the inelastic left Cauchy-Green deformation tensor  $\mathbf{C}_i^j$

$$\begin{aligned} \dot{\mathbf{C}}_i^j &= \frac{2}{\eta^j} \left[ 2\rho_0 \frac{\partial \Psi_{neq}^j}{\partial \mathbf{I}_{\mathbf{B}_e^j}} \mathbf{C} + 2\rho_0 \frac{\partial \Psi_{neq}^j}{\partial \Pi_{\mathbf{B}_e^j}} \left( \text{tr}(\mathbf{B}_e^j) \mathbf{C} - (\mathbf{F}_i^j)^T \cdot (\mathbf{C}_e^j \cdot \mathbf{C}_e^j) \cdot \mathbf{F}_i^j \right) \right. \\ &\quad \left. - \frac{1}{3} \text{tr} \left( 2\rho_0 \frac{\partial \Psi_{neq}^j}{\partial \mathbf{I}_{\mathbf{B}_e^j}} \mathbf{C}_e^j + 2\rho_0 \frac{\partial \Psi_{neq}^j}{\partial \Pi_{\mathbf{B}_e^j}} \left( \text{tr}(\mathbf{B}_e^j) \mathbf{C}_e^j - \mathbf{C}_e^j \cdot \mathbf{C}_e^j \right) \right) \mathbf{C}_i^j \right], \end{aligned} \quad (23)$$

which is reformulated with respect to the upcoming numerical implementation into

$$\begin{aligned} \dot{\mathbf{C}}_i^j &= \frac{2}{\eta^j} \left[ 2\rho_0 \frac{\partial \Psi_{neq}^j}{\partial \mathbf{I}_{\mathbf{B}_e^j}} \mathbf{C} + 2\rho_0 \frac{\partial \Psi_{neq}^j}{\partial \Pi_{\mathbf{B}_e^j}} \left( \text{tr}(\mathbf{C} \cdot (\mathbf{C}_i^j)^{-1}) \mathbf{C} - \mathbf{C} \cdot (\mathbf{C}_i^j)^{-1} \cdot \mathbf{C} \right) \right. \\ &\quad \left. - \frac{1}{3} \text{tr} \left( 2\rho_0 \frac{\partial \Psi_{neq}^j}{\partial \mathbf{I}_{\mathbf{B}_e^j}} \mathbf{C} \cdot (\mathbf{C}_i^j)^{-1} + 2\rho_0 \frac{\partial \Psi_{neq}^j}{\partial \Pi_{\mathbf{B}_e^j}} \left( \text{tr}(\mathbf{C} \cdot (\mathbf{C}_i^j)^{-1}) \mathbf{C} \cdot (\mathbf{C}_i^j)^{-1} - (\mathbf{C}_i^j)^{-1} \cdot \mathbf{C} \cdot (\mathbf{C}_i^j)^{-1} \cdot \mathbf{C} \right) \right) \mathbf{C}_i^j \right]. \end{aligned} \quad (24)$$

This provides the formulation of the evolution equation with respect to approaches based on polynomial series according to Eq. (2). The mathematical development of this formulation was kept general for alternative model approaches than in our case. In these considerations, there is no dependence on the second invariant  $\Pi_{\mathbf{B}_e^j}$ , so that the evolution equation is reduced to

$$\dot{\mathbf{C}}_i^j = \frac{4}{\eta^j} \rho_0 \frac{\partial \Psi_{neq}^j}{\partial \mathbf{I}_{\mathbf{B}_e^j}} \left[ \mathbf{C} - \frac{1}{3} \text{tr} \left( \mathbf{C} \cdot (\mathbf{C}_i^j)^{-1} \right) \mathbf{C}_i^j \right]. \quad (25)$$

Taking into account the free energies in (13) and (14), the evolution equation for the first Maxwell element is

$$\dot{\mathbf{C}}_i^1 = \frac{12}{r^1} (\mathbf{I}_{\mathbf{B}_e^1} - 3)^2 \left[ \mathbf{C} - \frac{1}{3} \text{tr} \left( \mathbf{C} \cdot (\mathbf{C}_i^1)^{-1} \right) \mathbf{C}_i^1 \right] \quad (26)$$

and for the remaining three Maxwell elements  $j = 2 \dots 4$

$$\dot{\mathbf{C}}_i^j = \frac{4}{r^j} \left[ \mathbf{C} - \frac{1}{3} \text{tr} \left( \mathbf{C} \cdot (\mathbf{C}_i^j)^{-1} \right) \mathbf{C}_i^j \right] \quad j = 2 \dots 4 \quad (27)$$

is obtained. In this equation, the parameter relaxation time  $r^j$  is introduced with

$$r^j = \frac{\eta^j}{c_{klj}}. \quad (28)$$

The pronounced non-linear behaviour, which can be seen under complicated conditions, is described by the usage of strain-dependent and strain rate-dependent relaxation times according to the work of Koprowski-Theiß (2011)

and Scheffer et al. (2013). Alternatively, the scaling of the viscosities is another possibility, cf. Rendek and Lion (2010). The norms of the inelastic Cauchy Green tensor  $\|\mathbf{C}_i^4\|$  and the deformation velocity  $\|\mathbf{D}\|$  are present in the expressions of the relaxation times  $r^j$ . They are chosen as

$$\begin{aligned}
r_1 &= r_{11}, \\
r_2 &= r_{21} + r_{22} \exp(-k_{21} \|\mathbf{D}\|), \\
r_3 &= r_{31} + r_{32} \exp(-k_{31} \|\mathbf{D}\|) + r_{33} \exp(-k_{32} \|\mathbf{D}\|), \\
r_4 &= r_{41} + (r_{42} + r_{43} \exp(-k_{41} \|\mathbf{D}\|)) (\|\mathbf{C}_i^4\| - \sqrt{3}).
\end{aligned} \tag{29}$$

The parameter  $r_{41}$  is determined as 0.1 s, or at least it has to be restricted being bigger than 0 s, to guarantee that the relaxation time does not vanish for static processes, in which the norm of  $\mathbf{C}_i$  equals  $\sqrt{3}$ . Otherwise, problems occur in the evaluation of the evolution equation (27), because it becomes singular.

### 3 Numerical realisation

The non-linear description in the given model and the consideration of large deformations some numerical utilities. The main focus of this contribution is the following comparison of two different realisations of the introduced model by numerical methods. Both provide advantages and disadvantages according to computational time and generality of the used formulation. The highest generality is given by the consideration of the complete three-dimensional model, provided in the last section. Its realisation is given in section 3.1. Subsequently, a reduction to special loading conditions, here for uniaxial tension, and the procedure for this realisation are given in 3.2. It has a higher performance with respect to computational time and can be used, if only restricted experimental data is available. Moreover, it is useful to get first information of the model's character and of the material parameters.

#### 3.1 FEM implementation

For the simulation of the mechanical behaviour of real structural components with complex geometries loaded under difficult conditions, the three-dimensional character of the model for large deformations is elementary. For the realisation, the finite element method (FEM) is necessary. According to the FEM, the whole Cauchy stress tensor  $\mathbf{T}$  has to be computed in each timestep  $t$ .

The starting point of the FEM calculation is the momentum balance

$$\rho \ddot{\mathbf{x}} = \operatorname{div} \mathbf{T} + \rho \mathbf{b}, \quad \text{respectively} \quad \operatorname{div} \mathbf{T} = 0 \tag{30}$$

in the absence of body forces  $\mathbf{b}$  and acceleration  $\ddot{\mathbf{x}}$ . After the multiplication with a test function  $\delta \mathbf{u}$  and integration by parts, this results in the so-called weak form

$$\int_{\Omega} \nabla \delta \mathbf{u} : \mathbf{T} \, d\Omega + \int_{\Gamma} \mathbf{t} \cdot \delta \mathbf{u} \, d\Gamma = 0 \tag{31}$$

of the momentum balance. To ensure the claimed incompressibility of the material, a secondary condition with an additional degree of freedom (DOF)  $\delta p$  has to be introduced

$$\int_{\Omega} \delta p (\det \mathbf{F} - 1) \, d\Omega = 0. \tag{32}$$

For numerical reasons, Taylor-Hood finite elements with quadratic shape functions for the displacement  $\mathbf{u}$  and linear functions for the pressure  $p$  have to be chosen.

To compare the results of the FEM calculation to those of the uniaxial reduction and the experiments, only Dirichlet boundary conditions are considered. The Neumann boundary term over the surface  $\Gamma$  vanishes. Due to the fact that the used constitutive equation (11) is strongly non-linear, an iterative method has to be accomplished to solve

$$f(\mathbf{u}, p) = \int_{\Omega} \nabla \delta \mathbf{u} : \mathbf{T} \, d\Omega + \int_{\Omega} \delta p (\det \mathbf{F} - 1) \, d\Omega = 0 \tag{33}$$

in every timestep. For the evaluation, functions  $\mathbf{u}(\mathbf{x})$  and  $p(\mathbf{x})$  have to be found for which this statement is true for all test functions  $\delta\mathbf{u}$  and  $\delta p$ . According to numerics, the approximations

$$\begin{aligned} u_{h,i}(\mathbf{x}) &= \sum_j U_j \varphi_j(\mathbf{x}) \quad \text{with } i = 1, 2, 3 \\ \text{and } p_h(\mathbf{x}) &= \sum_j P_j \psi_j(\mathbf{x}) \end{aligned} \quad (34)$$

are made, where  $U_j$  and  $P_j$  are the degrees of freedom of the problem,  $\varphi_j(\mathbf{x})$  and  $\psi_j(\mathbf{x})$  are the shape functions. In the following all discrete DOFs  $U_j$  and  $P_j$  are summed up in the vector  $\tilde{\mathbf{u}}$  for reasons of clarity and comprehensibility. Eq. (33) in combination with the approximations (34) results in

$$f_h(\tilde{\mathbf{u}}) = \int_{\Omega} \nabla \delta \mathbf{u}_h : \mathbf{T} \, d\Omega + \int_{\Omega} \delta p_h (\det \mathbf{F} - 1) \, d\Omega = 0. \quad (35)$$

For the implementation, the integral over  $\Omega = \cup \Omega_k$  is split into integrals over all  $l$  cells

$$\int_{\Omega} \nabla \delta \mathbf{u} : \mathbf{T} \, d\Omega + \int_{\Omega} \delta p (\det \mathbf{F} - 1) \, d\Omega = \sum_{k=1}^l \int_{\Omega_k} \nabla \delta \mathbf{u} : \mathbf{T} \, d\Omega_e + \sum_{k=1}^l \int_{\Omega_k} \delta p (\det \mathbf{F} - 1) \, d\Omega_e. \quad (36)$$

On each cell, its contribution is approximated by quadrature

$$\int_{\Omega_k} \nabla \delta \mathbf{u} : \mathbf{T} \, d\Omega_e + \int_{\Omega_k} \delta p (\det \mathbf{F} - 1) \, d\Omega_e = \sum_q \nabla \delta \mathbf{u} : \mathbf{T}(\mathbf{x}_q^k) w_q^k + \sum_q \delta p (\det \mathbf{F}(\mathbf{x}_q^k) - 1) w_q^k \quad (37)$$

where  $\mathbf{x}_q^k$  is the  $q^{\text{th}}$  quadrature point of cell  $k$  and  $w_q^k$  is the corresponding weight. Regarding Eq. (37) the stress-strain relation has to be evaluated at the integration points. A Taylor expansion yields a linear set of equations for all DOFs

$$\mathbf{K} \cdot \Delta \tilde{\mathbf{u}} = -\mathbf{f}(\tilde{\mathbf{u}}) \quad (38)$$

with the tangential stiffness matrix

$$\mathbf{K} = \frac{d\mathbf{f}(\tilde{\mathbf{u}})}{d\tilde{\mathbf{u}}} = \begin{pmatrix} \frac{\partial f_1}{\partial \tilde{u}_1} & \cdots & \frac{\partial f_1}{\partial \tilde{u}_n} \\ \frac{\partial f_2}{\partial \tilde{u}_1} & \cdots & \frac{\partial f_2}{\partial \tilde{u}_n} \\ \vdots & \ddots & \vdots \\ \frac{\partial f_n}{\partial \tilde{u}_1} & \cdots & \frac{\partial f_n}{\partial \tilde{u}_n} \end{pmatrix} \quad \text{or} \quad K_{ij} = \frac{\partial f_i(\tilde{\mathbf{u}})}{\partial \tilde{u}_j}. \quad (39)$$

Eq. (38) is solved iteratively and by updating the solution  $\tilde{\mathbf{u}}^{n+1} = \tilde{\mathbf{u}}^n + \Delta \tilde{\mathbf{u}}$  at the end of each step. The  $L_2$ -norm of the right-hand side of Eq. (38) serves as measurement for the solution's quality. Since the derivative is not easy to obtain, the so-called *numerical tangent* is used. Therefore, the differential quotient is replaced by the difference quotient

$$K_{ij} = \frac{\partial f_i(\tilde{\mathbf{u}})}{\partial \tilde{u}_j} = \frac{f_i(\tilde{\mathbf{u}}^j) - f_i(\tilde{\mathbf{u}})}{\epsilon_\alpha} \quad (40)$$

$$\text{with } \epsilon_\alpha \approx \delta_0(1 + |\tilde{u}_j|) \quad \text{and} \quad \tilde{\mathbf{u}}^j = \tilde{\mathbf{u}} + \epsilon_\alpha \mathbf{e}_j, \quad (41)$$

in which  $\delta_0$  in the variation  $\epsilon_\alpha$  is the square root of the tolerance of the used floating-point data type, cf. Pang (2006).

To consider the viscoelastic behaviour of the material, the used evolution equations have to be solved. Because of the non-linearity of Eq. (26) and (27), a local formulation at every integration point for every Maxwell element has to be used. For means of time discretisation, the Backward Euler method is reasonable. The non-linearity is considered by executing Newton's method again. Thus the rate of the inelastic right Cauchy-Green deformation tensor can be written as

$$\dot{\mathbf{C}}_i^j(t_{n+1}) \approx \frac{\mathbf{C}_i^j(t_{n+1}) - \mathbf{C}_i^j(t_n)}{\Delta t}. \quad (42)$$

This can be rewritten as the function

$$\begin{aligned} \mathbf{g}(\mathbf{C}_i^j(t_{n+1})) &= \frac{\mathbf{C}_i^j(t_{n+1}) - \mathbf{C}_i^j(t_n)}{\Delta t} - \dot{\mathbf{C}}_i^j(t_{n+1}) \\ &\stackrel{!}{=} \mathbf{0} \end{aligned} \quad (43)$$

for the calculation of the inelastic Cauchy-Green deformation tensor  $\mathbf{C}_i^j(t_{n+1})$  in the  $(n+1)^{\text{th}}$  timestep. Another Taylor expansion is performed

$$\mathbf{g}(\mathbf{C}_i^j(t_{n+1})) + \frac{\partial \mathbf{g}(\mathbf{C}_i^j(t_{n+1}))}{\partial \mathbf{C}_i^j(t_{n+1})} : \Delta(\mathbf{C}_i^j(t_{n+1})) \approx \mathbf{0}, \quad (44)$$

so that another set of equations is obtained

$$\mathbf{g}(\mathbf{C}_i^j(t_{n+1})) + \overset{4}{\mathbf{L}} : \Delta(\mathbf{C}_i^j(t_{n+1})) \approx \mathbf{0}, \quad (45)$$

and in analogy to Eq. (40) the differential quotient is replaced by the difference quotient

$$\Delta \mathbf{g} = \frac{\mathbf{g}(\mathbf{C}_i^j(t_{n+1})^{op}) - \mathbf{g}(\mathbf{C}_i^j(t_{n+1}))}{\epsilon_\beta}, \quad (46)$$

in which  $\mathbf{C}_i^j(t_{n+1})^{op}$  is the inelastic part of the right Cauchy-Green deformation tensor  $\mathbf{C}_i^j(t_{n+1})$  at timestep  $t_{n+1}$  and the current iteration step of the local Newton method, whose  $op^{\text{th}}$  component  $C_i^j(t_{n+1})_{op}$  has been modified by the variation  $\epsilon_\beta$

$$\mathbf{C}_i^j(t_{n+1})^{op} = \mathbf{C}_i^j(t_{n+1}) + \epsilon_\beta \delta_{ok} \delta_{pl} \mathbf{e}_k \otimes \mathbf{e}_l \quad (47)$$

with

$$\epsilon_\beta = \delta_0 \left( 1 + |C_i^j(t_{n+1})_{op}| \right). \quad (48)$$

This results in a rank four local tangential matrix with the components

$$\overset{4}{\mathbf{L}} \hat{=} L_{qrop} = \frac{g(\mathbf{C}_i^j(t_{n+1})^{op})_{qr} - g(\mathbf{C}_i^j(t_{n+1}))_{qr}}{\epsilon_\beta}. \quad (49)$$

This equation set can be solved and the tensor can be updated by

$$\Delta(\mathbf{C}_i^j(t_{n+1})) = \mathbf{C}_i^j(t_{n+1})^{k+1} - \mathbf{C}_i^j(t_{n+1})^k. \quad (50)$$

As the tolerance for the local Newton iteration, the Frobenius-Norm of  $\mathbf{g}(\mathbf{C}_i^j(t_{n+1}))$  is chosen, with

$$\|\mathbf{A}\| = \sqrt{\mathbf{A} : \mathbf{A}} = \sqrt{\sum_{i=1}^m \sum_{j=1}^n (a_{ij})^2}. \quad (51)$$

The presented relation set is realised in the open source FE library *deal.II*, cf. Bangerth et al. (2007, 2013).

This results in a complex simulation process, which is very time-consuming because of the non-linearities in the material's description. The strong coupling of the relaxation times in addition to this numerical effort yield a complex parameter identification process. Therefore, an alternative implementation method that is more effective in terms of parameter identification is introduced in the following .

### 3.2 Uniaxial reduction

In order to reduce the numerical effort, the introduced relations of the material model are reduced for the special case of the uniaxial tension test as also executed by Johlitz et al. (2010). The constitutive relation (15) for the Cauchy stress  $\mathbf{T}$  is evaluated for the case that the material is stretched with  $\lambda$  in the 1-direction. In this case, the transversal direction is stress-free

$$T_{22} = T_{33} = 0 \quad (52)$$

and the Lagrangian parameter  $p$  results in

$$\begin{aligned} p = & \left[ 2 c_{10} + 4 c_{20} (\text{tr}(\mathbf{B}) - 3) + 6 c_{30} (\text{tr}(\mathbf{B}) - 3)^2 \right] B_{22} \\ & + 6 c_{301} (\text{tr}(\mathbf{B}_e^1) - 3)^2 B_{e22}^1 + \sum_{j=2}^4 2 c_{10j} B_{e22}^j. \end{aligned} \quad (53)$$

A scalar-valued equation is obtained providing information that corresponds to the uniaxial experimental data

$$\begin{aligned}
T_{11} &= [2c_{10} + 4c_{20}(\text{tr}(\mathbf{B}) - 3) + 6c_{30}(\text{tr}(\mathbf{B}) - 3)^2] (B_{11} - B_{22}) \\
&\quad + 6c_{301}(\text{tr}(\mathbf{B}_e^1) - 3)^2 (B_{e_{11}}^1 - B_{e_{22}}^1) + \sum_{j=2}^4 2c_{10j} (B_{e_{11}}^j - B_{e_{22}}^j) \\
&= \left[ 2c_{10} + 4c_{20} \left( \lambda^2 + \frac{2}{\lambda} - 3 \right) + 6c_{30} \left( \lambda^2 + \frac{2}{\lambda} - 3 \right)^2 \right] \left( \lambda^2 - \frac{1}{\lambda} \right) \\
&\quad + 6c_{301} \left( (\lambda_e^1)^2 + \frac{2}{\lambda_e^1} - 3 \right)^2 \left( (\lambda_e^1)^2 - \frac{1}{\lambda_e^1} \right) + \sum_{j=2}^4 2c_{10j} \left( (\lambda_e^j)^2 - \frac{1}{\lambda_e^j} \right)
\end{aligned} \tag{54}$$

The relation of the stretches

$$\lambda = \lambda_e^j \lambda_i^j \quad \Leftrightarrow \quad \lambda_e^j = \frac{\lambda}{\lambda_i^j} \tag{55}$$

allows the reformulation of Eq. (54) as a function of  $\lambda$  and  $\lambda_i^j$

$$\begin{aligned}
T_{11} &= \left[ 2c_{10} + 4c_{20} \left( \lambda^2 + \frac{2}{\lambda} - 3 \right) + 6c_{30} \left( \lambda^2 + \frac{2}{\lambda} - 3 \right)^2 \right] \left( \lambda^2 - \frac{1}{\lambda} \right) \\
&\quad + 6c_{301} \left( \frac{\lambda^2}{(\lambda_i^1)^2} + \frac{2\lambda_i^1}{\lambda} - 3 \right)^2 \left( \frac{\lambda^2}{(\lambda_i^1)^2} - \frac{\lambda_i^1}{\lambda} \right) + \sum_{j=2}^4 2c_{10j} \left( \frac{\lambda^2}{(\lambda_i^j)^2} - \frac{\lambda_i^j}{\lambda} \right).
\end{aligned} \tag{56}$$

The evolution equations for the inelastic deformations in the different Maxwell elements also have to be specified with respect to the uniaxial case. This procedure is accomplished in detail once for the first Maxwell element with

$$\dot{\mathbf{C}}_i^1 = \frac{12}{r^1} (\mathbf{I}_{\mathbf{B}_e^1} - 3)^2 \left[ \mathbf{C} - \frac{1}{3} \text{tr}(\mathbf{C} \cdot (\mathbf{C}_i^1)^{-1}) \mathbf{C}_i^1 \right], \tag{57}$$

which denotes for the uniaxial case

$$\begin{aligned}
\dot{\mathbf{C}}_i^1 &= \frac{d}{dt} \mathbf{C}_i^1 \hat{=} \begin{bmatrix} 2\lambda_i^1 \dot{\lambda}_i^1 & 0 & 0 \\ 0 & -\frac{\dot{\lambda}_i^1}{(\lambda_i^1)^2} & 0 \\ 0 & 0 & -\frac{\dot{\lambda}_i^1}{(\lambda_i^1)^2} \end{bmatrix} \\
&= \frac{12 \left( \frac{\lambda^2}{(\lambda_i^1)^2} + \frac{2\lambda_i^1}{\lambda} - 3 \right)^2}{r^1} \left( \begin{bmatrix} \lambda^2 & 0 & 0 \\ 0 & \frac{1}{\lambda} & 0 \\ 0 & 0 & \frac{1}{\lambda} \end{bmatrix} - \frac{1}{3} \frac{\lambda^3 + 2(\lambda_i^1)^3}{(\lambda_i^1)^2 \lambda} \begin{bmatrix} (\lambda_i^1)^2 & 0 & 0 \\ 0 & \frac{1}{\lambda_i^1} & 0 \\ 0 & 0 & \frac{1}{\lambda_i^1} \end{bmatrix} \right).
\end{aligned} \tag{58}$$

These equations must be identical. Thus, the evolution equation for the first component remains

$$\begin{aligned}
2\lambda_i^1 \dot{\lambda}_i^1 &= \frac{12 \left( \frac{\lambda^2}{(\lambda_i^1)^2} + \frac{2\lambda_i^1}{\lambda} - 3 \right)^2}{r^1} \left[ \lambda^2 - \frac{1}{3} \frac{\lambda^3 + 2(\lambda_i^1)^3}{\lambda} \right] \\
\Leftrightarrow \dot{\lambda}_i^1 &= \frac{4}{r^1} \left( \frac{\lambda^2}{(\lambda_i^1)^2} + \frac{2\lambda_i^1}{\lambda} - 3 \right)^2 \left( \lambda^2 - \frac{(\lambda_i^1)^2}{\lambda} \right).
\end{aligned} \tag{59}$$

This non-linear equation can be solved by means of a Backward Euler scheme in the time with the differential quotient

$$\dot{\lambda}_i^1 \approx \frac{\lambda_i^1(t_{n+1}) - \lambda_i^1(t_n)}{\Delta t} = \frac{4}{r^1} \left( \frac{\lambda^2(t_{n+1})}{(\lambda_i^1(t_{n+1}))^2} + \frac{2\lambda_i^1(t_{n+1})}{\lambda(t_{n+1})} - 3 \right)^2 \left( \frac{\lambda(t_{n+1})^2}{\lambda_i^1(t_{n+1})} - \frac{\lambda_i^1(t_{n+1})^2}{\lambda(t_{n+1})} \right). \tag{60}$$

In this equation,  $\Delta t$  is the time step between time iteration  $t_n$  and  $t_{n+1}$ . The developed non-linear equation (60) is rewritten as a function of  $f((\lambda_i^j)^k(t_{n+1}))$

$$\begin{aligned} f((\lambda_i^1)^k(t_{n+1})) &= \lambda_i^1(t_{n+1}) - \lambda_i^1(t_n)\Delta t \\ &\quad - \frac{4\Delta t}{r^1} \left( \frac{\lambda(t_{n+1})^2}{\lambda_i^1(t_{n+1})^2} + \frac{2\lambda_i^1(t_{n+1})}{\lambda(t_{n+1})} - 3 \right)^2 \left( \frac{\lambda(t_{n+1})^2}{\lambda_i^1(t_{n+1})} - \frac{\lambda_i^1(t_{n+1})^2}{\lambda(t_{n+1})} \right) \\ &= 0, \end{aligned} \quad (61)$$

and formally linearised for the Newton procedure

$$f((\lambda_i^1)^k(t_{n+1})) + \frac{\partial f((\lambda_i^1)^k(t_{n+1}))}{\partial (\lambda_i^1)^k(t_{n+1})} ((\lambda_i^1)^{k+1}(t_{n+1}) - (\lambda_i^1)^k(t_{n+1})) = 0, \quad (62)$$

in which the derivative of the function represents the tangent stiffness  $K_T^1$

$$\begin{aligned} K_T^1 &= \frac{\partial f((\lambda_i^1)^k(t_{n+1}))}{\partial (\lambda_i^1)^k(t_{n+1})} \\ &= 1 + \frac{4\Delta t}{r^1} \left( \frac{\lambda^2}{\lambda_i^1} - \frac{(\lambda_i^1)^2}{\lambda} \right) \left( \frac{4\lambda^4}{(\lambda_i^1)^5} + \frac{4\lambda}{(\lambda_i^1)^2} - \frac{8\lambda_i^1}{\lambda^2} - \frac{12\lambda^2}{(\lambda_i^1)^3} + \frac{12}{\lambda} \right) \\ &\quad + \frac{4\Delta t}{r^1} \left( \frac{\lambda^2}{(\lambda_i^1)^2} + \frac{2\lambda_i^1}{\lambda} - 3 \right)^2 \left( \frac{\lambda^2}{(\lambda_i^1)^2} - \frac{2\lambda_i^1}{\lambda} \right). \end{aligned} \quad (63)$$

In order to shorten the notation of Eq. (63), the term  $(t_{n+1})$  is omitted. All the stretches  $\lambda$  and  $\lambda_i^1$  have to be evaluated with respect to the time step  $(t_{n+1})$ . The index  $k$  within the equation stands for the iteration index in the Newton method. The increment of the update is computed to

$$\Delta\lambda_i^1(t_{n+1}) = (\lambda_i^1)^{k+1}(t_{n+1}) - (\lambda_i^1)^k(t_{n+1}) = -\frac{f((\lambda_i^j)^k(t_{n+1}))}{K_T^1}, \quad (64)$$

which results in

$$(\lambda_i^1)^{k+1}(t_{n+1}) = (\lambda_i^1)^k(t_{n+1}) + \Delta\lambda_i^1(t_{n+1}). \quad (65)$$

The procedure for the other Maxwell elements ( $j = 2\dots 4$ ) has to be executed analogously. The resulting equations for these elements are

$$\begin{aligned} \dot{\lambda}_i^j &= \frac{4}{3r^j} \left( \frac{\lambda^2}{\lambda_i^j} - \frac{(\lambda_i^j)^2}{\lambda} \right) \\ f((\lambda_i^j)^k(t_{n+1})) &= (\lambda_i^j)^k(t_{n+1}) - \lambda_i^j(t_n) - \frac{4\Delta t}{3r^j} \left[ \frac{\lambda^2(t_{n+1})}{(\lambda_i^j)^k(t_{n+1})} - \frac{((\lambda_i^j)^k(t_{n+1}))^2}{\lambda(t_{n+1})} \right] = 0 \\ K_T^j &= 1 + \frac{4\Delta t}{3r^j} \left[ \frac{\lambda^2(t_{n+1})}{((\lambda_i^j)^k(t_{n+1}))^2} + \frac{2(\lambda_i^j)^k(t_{n+1})}{\lambda(t_{n+1})} \right]. \end{aligned} \quad (66)$$

In addition, attention has to be paid to the non-linearities of the relaxation times for this scalar realisation. Therefore, the norm of the deformation velocity  $\|\mathbf{D}\|$  is reduced to

$$\|\mathbf{D}\| = \sqrt{\frac{3}{2}} \frac{\dot{\lambda}}{\lambda} \quad (67)$$

and according to the fourth relaxation time,  $\|\mathbf{C}_i^4\|$  is

$$\|\mathbf{C}_i^4\| = \sqrt{(\lambda_i^4)^4 + \frac{2}{(\lambda_i^4)^2}} \quad (68)$$

for the observed uniaxial case. The residue of the function  $f((\lambda_i^j)^k(t_{n+1}))$  as the tolerance of the Newton scheme is chosen as  $10^{-8}$  for all evolution equations. This procedure with the presented equations is implemented in Matlab<sup>®</sup>, which also provides the tools for the parameter identification, in this case by a genetic algorithm.

The parameter identification delivers the following values for the basic elasticity (Table 1) and the viscoelastic

Table 1: Identified parameters with respect to the basic elasticity.

$c_{10}$	$c_{20}$	$c_{30}$
[MPa]	[MPa]	[MPa]
0.2	-0.052	0.017

Table 2: Identified parameters with respect to the viscoelasticity.

$c_{301}$	0.002 MPa	$c_{102}$	0.057 MPa
$r_I$	$10^6$ s	$r_{21}$	40.0 s
		$r_{22}$	4000.0 s
		$k_{21}$	$10^{14}$ s
$c_{103}$	0.061 MPa	$c_{104}$	3.0 MPa
$r_{31}$	23 s	$r_{41}$	0.1 s
$r_{32}$	529 s	$r_{42}$	0.22 s
$k_{31}$	32.08 s	$r_{43}$	20.74 s
$r_{33}$	400000 s	$k_{41}$	131.82 s
$k_{32}$	$10^{14}$ s		

parameters (Table 2), respectively. Details of the identification can be found in Koprowski-Theiß et al. (2011b). The  $c_{20}$ -parameter has to be negative in the present case to represent the characteristic *S*-shaped basic elasticity with the initial decrease and subsequent increase of the material's stiffness for increasing deformations, according to the work of Yeoh and Fleming (1997) and Dhondt (2004). For the uniaxial deformations, Drucker stability is still fulfilled for  $\lambda \in ]0; \infty[$  (cf. Drucker (1957)). The numerical effort compared to the three-dimensional implementation in section 3.1 is significantly higher. In this case, an equation set has to be solved contrary to the single equation for the 1-direction. Furthermore, the global Newton scheme does not have to be applied for the scalar solution.

## 4 Results

The given numerical realisations with respect to the presented non-linear material model are now compared according to the experimental results. For the cyclic tests for different strain rates, the data set is restricted to one and a half loading cycles for reasons of clarity. The numerical results for both implementations match perfectly, see Fig. 2.

The results for the relaxation test match as well, in this case for the example of a relaxation experiment over 6000 s for  $\lambda = 1.6$ , see Fig. 3.

## 5 Conclusions

In this contribution, a non-linear viscoelastic material model representing the mechanical behaviour of a carbon black-filled EPDM is introduced. A major point in the material model is the representation of the non-linearities by non-linear relaxation times. The resulting complexity of the model itself yields high computational effort. Two different strategies in the numerical realisation are provided. At first, the implementation in the open source FE library *deal.II* was presented. Because of its complex equation setup, it is not very effective due to the high amount of computational time, whereby the numerical potential with respect to multiaxiality is provided completely. For reasons of effectivity in the parameter identification, as another numerical solution, the model has been implemented for the restricted case of uniaxial tension. This restriction denotes a strict limitation of the model neglecting all other conditions but the simple uniaxial case.

These results and the advantages and disadvantages in numerics are very important with respect to future work. Therein more complex loading conditions or real assemblies shall be investigated. The necessity of a multiaxial observation is illustrated in Johlitz and Diebels (2011) and Seibert et al. (2014). Therefore, the complete three-dimensional information is necessary, and the given FEM-solution has to be executed with an inverse identification process to get the model parameters. However, as a first step, uniaxial tests and the uniaxial reduction of the model can provide first ideas of the model's structure and the parameter range.

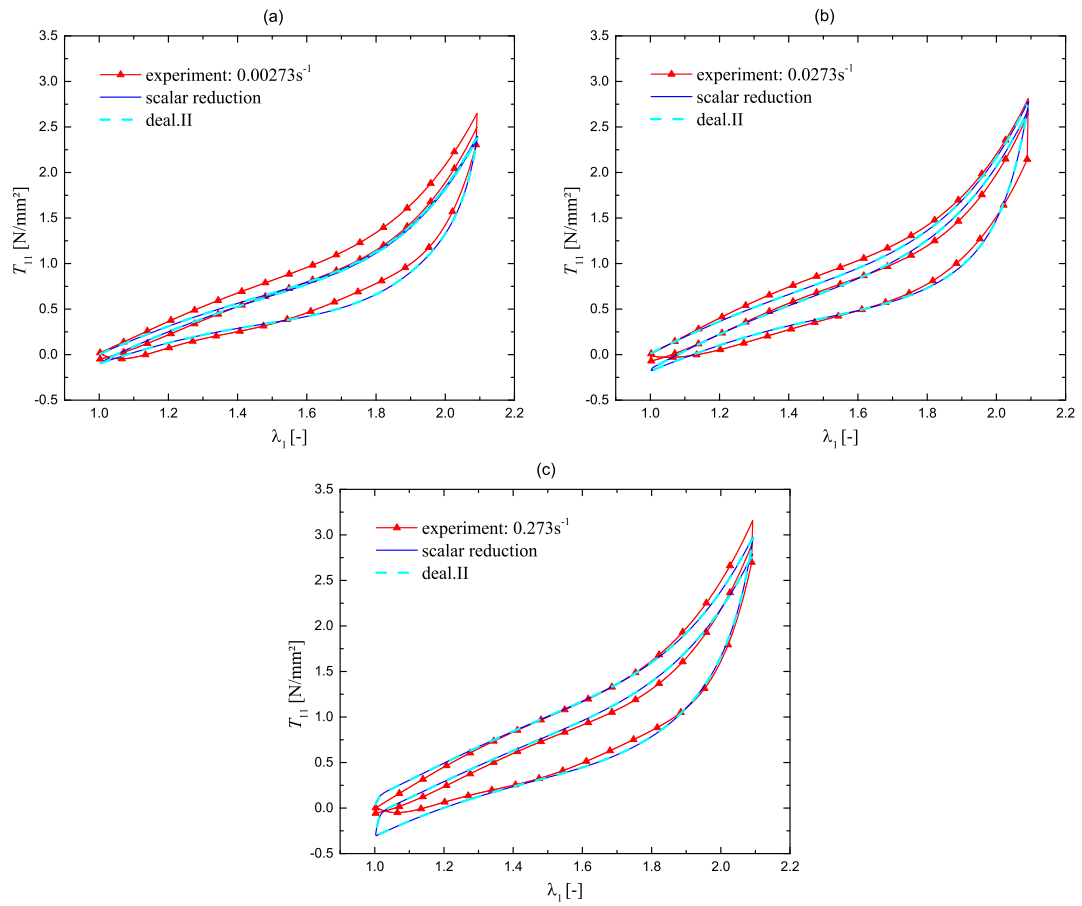


Figure 2: Cyclic tests with different strain rates: a)  $0.00273 \text{ s}^{-1}$ , b)  $0.0273 \text{ s}^{-1}$ , c)  $0.273 \text{ s}^{-1}$ ; comparison of the experiment and the numerical results.

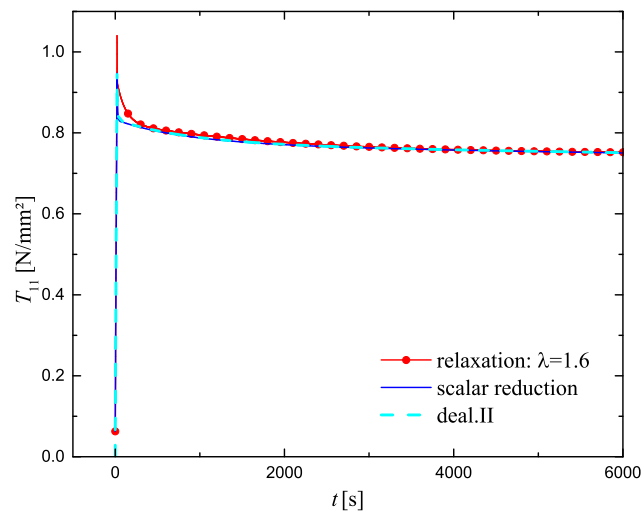


Figure 3: Relaxation experiment for  $\lambda = 1.6$ ; experiment and numerical results.

## References

- Amin, A.; Lion, A.; Höfer, P.: Effect of temperature history on the mechanical behaviour of a filler-reinforced NR/BR blend: Literature review and critical experiments. *Z. Angew. Math. Mech.*, 90, 5, (2010), 347–369.
- Amin, A.; Lion, A.; Sekita, S.; Okui, Y.: Nonlinear dependence of viscosity in modeling the rate-dependent response of natural and high damping rubbers in compression and shear: Experimental identification and numerical verification. *Int. J. Plast.*, 22, 9, (2006), 1610–1657.
- Bangerth, W.; Hartmann, R.; Kanschä, G.: deal.II – a General Purpose Object Oriented Finite Element Library. *ACM Trans. Math. Softw.*, 33, 4, (2007), 24/1–24/27.
- Bangerth, W.; Heister, T.; Heltai, L.; Kanschä, G.; Kronbichler, M.; Maier, M.; Turcksin, B.; Young, T. D.: The deal.II Library, Version 8.1. *arXiv preprint*.
- Besdo, D.; Ihlemann, J.: A phenomenological constitutive model for rubberlike materials and its numerical applications. *Int. J. Plast.*, 19, 7, (2003), 1019–1036.
- Bowen, R.: Theory of mixtures, AC Eringen. *Continuum Physics, Academic Press, New York*.
- Coleman, B.; Noll, W.: The thermodynamics of elastic materials with heat conduction and viscosity. *Arch. Ration. Mech. Anal.*, 13, 1, (1963), 167–178.
- Dannenberg, E.: Effects of surface chemical interactions on the properties. *Rubber Chem. Technol.*, 48, 3, (1975), 410–444.
- de Boer, R.; Ehlers, W.: *Theorie der Mehrkomponentenkontinua mit Anwendung auf bodenmechanische Probleme*. Univ.-Gesamthochschule (1986).
- Dhondt, G.: *The finite element method for three-dimensional thermomechanical applications*. John Wiley & Sons (2004).
- Drucker, D. C.: A definition of stable inelastic material. Tech. rep., DTIC Document (1957).
- Hartmann, S.; Tschöpe, T.; Schreiber, L.; Haupt, P.: Finite deformations of a carbon black-filled rubber. Experiment, optical measurement and material parameter identification using finite elements. *Eur. J. Mech. A. Solids*, 22, 3, (2003), 309–324.
- Haupt, P.: *Continuum mechanics and theory of materials*. Springer (2000).
- Haupt, P.; Lion, A.: On finite linear viscoelasticity of incompressible isotropic materials. *Acta Mech.*, 159, 1-4, (2002), 87–124.
- Johlitz, M.: *Experimentelle Untersuchung und Modellierung von Maßstabeffekten in Klebungen*, vol. 12 of *Saarbrücker Reihe Materialwissenschaft und Werkstofftechnik*. Shaker (2009).
- Johlitz, M.; Diebels, S.: Characterisation of a polymer using biaxial tension tests. Part I: Hyperelasticity. *Arch Appl. Mech.*, 81, 10, (2011), 1333–1349.
- Johlitz, M.; Scharding, D.; Diebels, S.; Retka, J.; Lion, A.: Modelling of thermo-viscoelastic material behaviour of polyurethane close to the glass transition temperature. *Z. Angew. Math. Mech.*, 90, 5, (2010), 387–398.
- Kaliske, M.; Rothert, H.: Constitutive approach to rate-independent properties of filled elastomers. *Int. J. Solids Struct.*, 35, 17, (1998), 2057–2071.
- Keck, J.: *Zur Beschreibung finiter Deformationen von Polymeren: Experimente, Modellbildung, Parameteridentifikation und Finite-Elemente-Formulierung*. Universität Stuttgart (1998).
- Koprowski-Theiß, N.: *Kompressible, viskoelastische Werkstoffe: Experimente, Modellierung und FE-Umsetzung*, vol. 25 of *Saarbrücker Reihe Materialwissenschaft und Werkstofftechnik*. Shaker (2011).
- Koprowski-Theiß, N.; Johlitz, M.; Diebels, S.: Characterizing the time dependence of filled EPDM. *Rubber Chem. Technol.*, 84, 2, (2011a), 147–165.
- Koprowski-Theiß, N.; Johlitz, M.; Diebels, S.: Modelling of a cellular rubber with nonlinear viscosity functions. *Exp. Mech.*, 51, 5, (2011b), 749–765.

- Koprowski-Theiß, N.; Johlitz, M.; Diebels, S.: Compressible rubber materials: Experiments and simulations. *Arch Appl. Mech.*, 82, 8, (2012a), 1117–1132.
- Koprowski-Theiß, N.; Johlitz, M.; Diebels, S.: Pressure dependent properties of a compressible polymer. *Exp. Mech.*, 52, 3, (2012b), 257–264.
- Kröner, E.: Allgemeine Kontinuumstheorie der Versetzungen und Eigenspannungen. *Archive for Rational Mechanics and Analysis*, 4, 1, (1959), 273–334.
- Laiarinandrasana, L.; Piques, R.; Robisson, A.: Visco-hyperelastic model with internal state variable coupled with discontinuous damage concept under total Lagrangian formulation. *Int. J. Plast.*, 19, 7, (2003), 977–1000.
- Lee, E.: Elastic-plastic deformation at finite strains. *J. Appl. Mech.*, 36, (1969), 1.
- Lion, A.: A constitutive model for carbon black filled rubber: Experimental investigations and mathematical representation. *Continuum Mech. Thermodyn.*, 8, 3, (1996), 153–169.
- Lion, A.: *Thermomechanik von Elastomeren*. Berichte des Institut für Mechanik 1/2000, Universität Kassel (2000).
- Lion, A.: Phenomenological modelling of the material behaviour of carbon black-filled rubber in continuum mechanics. *KGK Kautsch. Gummi Kunstst.*, 57, 4, (2004), 184–190.
- Marckmann, G.; Verron, E.: Comparison of hyperelastic models for rubber-like materials. *Rubber Chem. Technol.*, 79, 5, (2006), 835–858.
- Miehe, C.; Keck, J.: Superimposed finite elastic-viscoelastic-plastoelastic stress response with damage in filled rubbery polymers. Experiments, modelling and algorithmic implementation. *J. Mech. Phys. Solids*, 48, 2, (2000), 323–365.
- Pang, T.: *An Introduction to Computational Physics*. Cambridge University Press (2006).
- Reese, S.: *Thermomechanische Modellierung gummiartiger Polymerstrukturen*. Institut für Baumechanik und Numerische Mechanik, Hannover (2000).
- Reese, S.; Govindjee, S.: A theory of finite viscoelasticity and numerical aspects. *Int. J. Solids Struct.*, 35, 26-27, (1998), 3455–3480.
- Rendek, M.; Lion, A.: Strain induced transient effects of filler reinforced elastomers with respect to the payne-effect: Experiments and constitutive modelling. *Z. Angew. Math. Mech.*, 90, 5, (2010), 436–458.
- Rivlin, R. S.; Saunders, D.: Large elastic deformations of isotropic materials. VII. Experiments on the deformation of rubber. *Philosophical Transactions of the Royal Society of London A: Mathematical, Physical and Engineering Sciences*, 243, 865, (1951), 251–288.
- Scheffer, T.; Seibert, H.; Diebels, S.: Optimisation of a pretreatment method to reach the basic elasticity of filled rubber materials. *Arch. Appl. Mech.*, 83, 11, (2013), 1659–1678.
- Sedlan, K.: *Viskoelastisches Materialverhalten von Elastomerwerkstoffen: Experimentelle Untersuchung und Modellbildung*. Berichte des Institut für Mechanik 2/2001, Universität Kassel (2001).
- Seibert, H.; Scheffer, T.; Diebels, S.: Biaxial testing of elastomers - Experimental setup, measurement and experimental optimisation of specimen's shape. *Technische Mechanik*, 34, 2, (2014), 72–89.
- Truesdell, C.; Noll, W.: *The non-linear field theories of mechanics*. Springer (2004).
- Truesdell, C.; Toupin, R.: *The classical field theories*. Springer (1960).
- Yeoh, O.: Some forms of the strain energy function for rubber. *Rubber Chem. Technol.*, 66, 5, (1993), 754–771.
- Yeoh, O.; Fleming, P.: A new attempt to reconcile the statistical and phenomenological theories of rubber elasticity. *J. Polym. Sci., Part B: Polym. Phys.*, 35, 12, (1997), 1919–1931.

---

*Address:*

*corresponding author:*

Dipl.-Ing. Tobias Scheffer

Lehrstuhl für Technische Mechanik, Universität des Saarlandes, Campus, A 4.2, D - 66123 Saarbrücken

email: [t.scheffer@mx.uni-saarland.de](mailto:t.scheffer@mx.uni-saarland.de)

Dr.-Ing. Florian Goldschmidt

Lehrstuhl für Technische Mechanik, Universität des Saarlandes, Campus, A 4.2, D - 66123 Saarbrücken

email: [f.goldschmidt@mx.uni-saarland.de](mailto:f.goldschmidt@mx.uni-saarland.de)

Prof. Dr.-Ing. Stefan Diebels

Lehrstuhl für Technische Mechanik, Universität des Saarlandes, Campus, A 4.2, D - 66123 Saarbrücken

email: [s.diebels@mx.uni-saarland.de](mailto:s.diebels@mx.uni-saarland.de)